Sensors & Actuators: B. Chemical 283 (2019) 255–261

Contents lists available at ScienceDirect

Sensors and Actuators B: Chemical

journal homepage: www.elsevier.com/locate/snb

An ultrastable magnesium-organic framework as multi-responsive luminescent sensor for detecting trinitrotoluene and metal ions with high selectivity and sensitivity

Jin-Song Hu[a,b,c,*], Sheng-Ju Dong[a], Ke Wu[a], Xiao-Long Zhang[a], Jian Jiang[a], Jia Yuan[a], Ming-Dong Zheng[a,**]

[a] School of Chemical Engineering, Anhui University of Science and Technology, Huainan 232001, PR China
[b] Hefei Institute of Physical Science, Chinese Academy of Sciences, PR China
[c] Key Laboratory of Photochemical Conversion and Optoelectronic Material, TIPC, CAS, PR China

ARTICLE INFO

Keywords:
Metal organic frameworks
2,4,6-Trinitrotoluene
Metal ions
Fluorescence sensing

ABSTRACT

A pH and thermal stable three dimensional framework $[Mg(ATDC)(H_2O)_2]_n$ (**1**) (H_2ATDC = 2′-amino-1,1′:4′,1″-terphenyl-4,4″-dicarboxylate) with blue fluorescence has been successfully synthesized and characterized. The Mg-MOF contains 2D $[Mg(COO)_2]_n$ sheet, which links $ATDC^{2-}$ to generate 3D framework with accessible -NH_2 groups, which could be beneficial to impact the reorganization on specific small molecules. Importantly, it is the first reported highly selective fluorescence Mg-MOF for sensing 2,4,6-Trinitrotoluene (TNT), and have the highest sensitivity for detecting Chromium(III) simultaneously through fluorescence quenching. Furthermore, the quenching mechanisms are mainly attributed to the photo-induced electron transfer and competitive absorptions between the excitation/emission of Mg-MOF and analytes, rather than the interactions between –NH_2 and analytes.

1. Introduction

Nowdays, how to rapidly detect hazardous organic and heavy metal ions has been an important challenge for environmental protection [1,2], homeland security [3,4] and human health [5–7]. The hazardous nitro aromatic explosives (NAEs) are important materials of industrial explosives [8], especially for TNT, it can lead to potential explosion hazard and soil/aquatic pollution when be released into the environment [9]. Similarly, chromium(III) is one of the hazardous metal pollutants since it is a threat to the environment and toxic to human health [10,11], the excess Cr^{3+} also can lead to mutations and cancers [12,13]. However, some current commercial detecting techniques, such as nuclear magnetic resonance (NMR) [14], atomic absorption spectrometry (AAS) [3], mass spectrometry (MS) [15] and so on, are difficult to meet the needs of the real-time detection because of the complication and time-consuming. Therefore, it is a challenging research issue to explore new methods for rapidly and selectively detecting NAEs and heavy-metal ions easily and real-time.

Currently, luminescent MOFs (LMOFs) have received some attentions as chemical sensors because of their high selectivity and sensitivity, quick response, and recoverability [16,17]. As far as we know, there are many LMOFs as sensors for sensing nitro aromatic compounds and heavy-metal ions, mainly for sensing NB and TNP [18,19], but it hasn't been reported yet for high selectively sensing TNT, so it is a significative challenge to develop new LMOFs sensors for detecting it. In fact, a good number of LMOFs thus far were built by the lanthanide or transition-metal ions [20,21], the alkaline-earth LMOFs have been rarely explored for detecting NAEs and heavy-metal ion due to the difficulties of synthesis and application [22,23]. Recently, we are interested our research in constructing Mg^{2+} based MOFs and exploring their applications on luminescent sensing. Combination of the low toxicity of alkali metals and our research work, a rigid rich electronic ligand H_2ATDC (2′-amino-1,1′:4′,1″-terphenyl-4,4″-dicarboxylate) with active –NH_2 groups was selected to construct multifunctional Mg^{2+}-based luminescent sensors. Here, a pH and thermo stable three dimensional framework $[Mg(ATDC)(H_2O)_2]_n$ (**1**) with blue fluorescence was prepared, the Mg-MOF contains 2D $[Mg(COO)_2]_n$ sheet, which linked $ATDC^{2-}$ to generate 3D framework with accessible -NH_2 groups, which could be beneficial to sense small molecules. Fluorescence studies show that the Mg-MOF is the first reported recyclable highly

* Corresponding author at: School of Chemical Engineering, Anhui University of Science and Technology, Huainan 232001, PR China.
** Corresponding author.
E-mail addresses: jshu@aust.edu.cn (J.-S. Hu), mdzheng@aust.edu.cn (M.-D. Zheng).

https://doi.org/10.1016/j.snb.2018.12.022
Received 8 June 2018; Received in revised form 3 December 2018; Accepted 5 December 2018
Available online 05 December 2018
0925-4005/

selective fluorescence sensor for detecting TNT, and the highest sensitive fluorescence sensor for detecting Cr(III) simultaneously through fluorescence quenching. Furthermore, the quenching mechanisms were also well studied, the sensing properties were mainly attributed to the competitive absorptions between the analytes and excitation/ emission of Mg-MOF, rather than the interactions of weak bondings.

2. Experimental

2.1. Synthesis of Mg-MOF 1

The reactants of H_2ATDC(0.1 mmol, 0.42 g), $Mg(NO_3)_2{\cdot}6H_2O$ (0.1 mmol, 0.26 g) were dissolved in 10 mL of DMF/MeOH/H_2O (2:1:1, v/v), 2 drops HCl solution (1 mol/L) was added dropwise. The final suspension was sealed in a Parr Teflon-lined stainless steel reaction kettle (15 mL) and heated at 90 °C for 4 days, then cooled to room temperature slowly, light brown block crystals of **1** were obtained in 75% yield by centrifuging and washing two times (based on H_2ATDC). Anal. Calcd for $C_{80}H_{60}O_{18}N_4Mg$: C, 69.15, H, 4.32, N, 4.03; found C, 69.02, H, 4.50, N, 4.27. IR (KBr, cm^{-1}): 3450(s), 3360(s), 3030(m), 1590(vs), 1540(vs), 1390(vs), 1190(m), 1140(m), 1000(m), 791(s), 640(b), 540(s).

3. Results and discussion

3.1. Crystal structure discussions

The space group of **1** is $P2_1/c$, the building unit contains one $ATDC^{2-}$ anion, one Mg(II) cation and two coordinated water molecules (Table S1 and S2). The Mg(II) center has an octahedral coordination geometry composed by four other O atoms contributing from four different $ATDC^{2-}$ in the equatorial plane, and two O atoms of H_2O in the axis (Fig. 1a). In complex **1**, each COO- linked two Mg(II) to generate a 2D sheet, the coordinated water hang up and down of the sheet (Fig. 1b). Then the $ATDC^{2-}$ linked the adjacent sheets to form a 3D framework with rectangular channels and available -NH_2 groups (Fig. 1c).

3.2. Thermogravimetric analyses and PXRD patterns

To evaluate the thermo stability of **1**, TGA plot has been measured under N_2 atmosphere and is shown in Fig. S1. The result reveals that complex **1** has not weight loss at 35–160 °C, then it has a weight loss of 9.0% at the range of 160–225 °C, which attributes to the departure of coordinated water molecules (calcd 9.2%), the framework start to decompose up to 550 °C, showing the high thermal stability. As shown in Fig. S2, the PXRD diffraction peaks of the experimental are completely consistent with the stimulated, showing the high purity of complex **1**.

3.3. Fluorescence properties

The solid luminescence excitation and emission spectra of the H_2ATDC and complex **1** have been measured at ambient temperature. As shown in Fig. S3, the free H_2ATDC shows a broad emission with the fluorescence peak at 500 nm (λ_{ex} = 350 nm), and complex **1** show an intensive emission with the fluorescence peak at 460 nm (λ_{ex} = 380 nm). Complex **1** shows superior fluorescence intensity and a slight blue shift of approximately 40 nm than H_2ATDC, which is attributed to tightly stacking and the ligand to ligand charge transfer, therefore has widely applications in luminescent sensing [21].

3.4. pH stability properties

The stabilities of complex **1** at different pH conditions were studied at ambient temperature as well, the fluorescence intensities of **1** were measured after treating with aqueous solution of various pH values for 10 h, the results show the fluorescence intensities haven't obviously changed when pH values changed from 1 to 12. Further PXRD

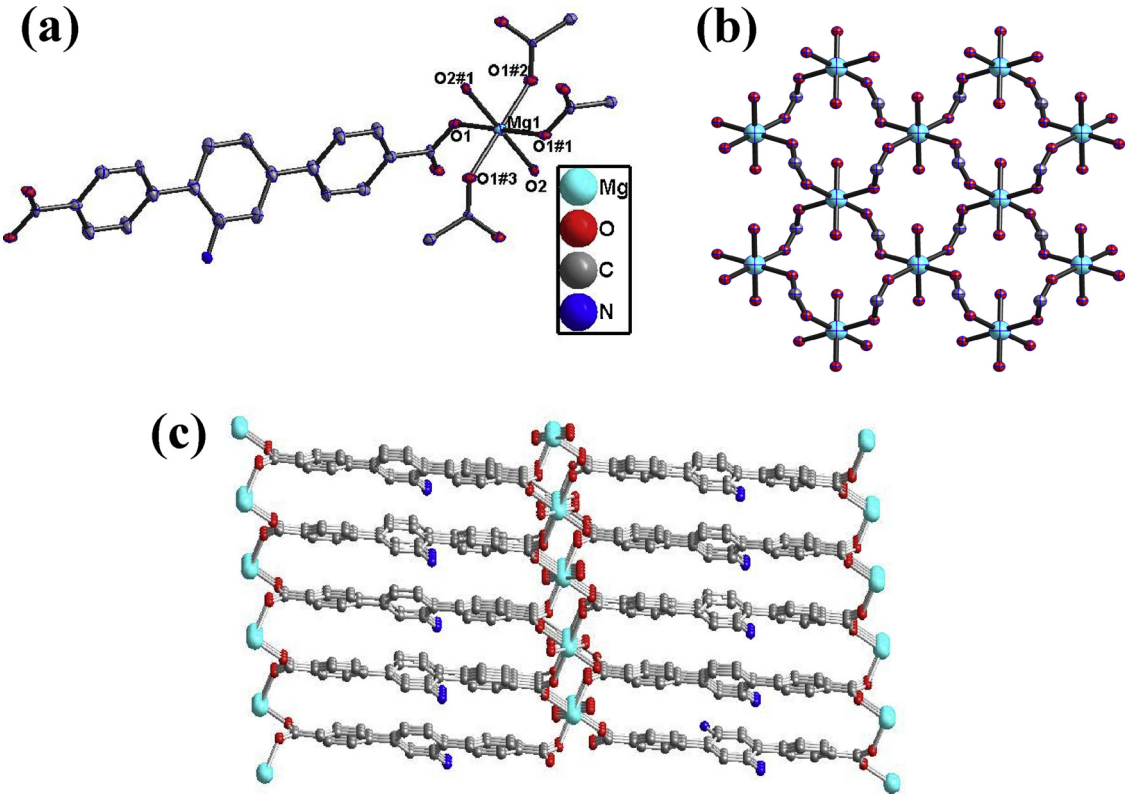

Fig. 1. (a) Coordination environment of Mg(II), #1 = 1-*x*, 1-*y*, 1-*z*; #2 = 1-*x*, -0.5+*y*, 1.5-*z*; #3 = *x*, 1.5-*y*, -0.5+*z*; (b) Each COO^- linked two Mg(II) to generate 2D sheet; (c) Three dimensional framework constructed by $ATDC^{2-}$ linking the adjacent sheets.

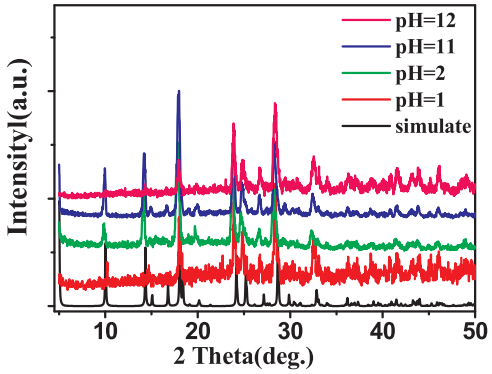

Fig. 2. PXRD patterns of **1** in various pH values (1, 2, 11, 12).

characterizations also confirmed the stabilities of complex **1** in different pH values (pH = 1–12) (Fig. 2 and S4).

3.5. Selective sensing of nitro-explosive compounds and cations

When H_2ATDC is coordinated to Mg^{2+} ion, fluorescence intensity is rapidly enhanced, which attribute to the enhancement of rigidity and the π-conjugacy of the H_2ATDC. Considering the excellent photoluminescence and thermal/pH stabilities, it is hoped to explore the potential fluorescence performances for detecting nitro-explosive compounds and metal ions. The emission spectrum of **1** indicates that complex **1** can be well-dispersed in most solvents such as DMA, DMF, CH_2Cl_2, EtOH, MeOH and THF to form stable suspension liquids, complex **1** displays stronger luminescent intensity in DMF, CH_3CN and CH_3OH, while exhibiting weaker intensity in water (Fig. S5). Consideration of the solubilities of analytes and the stable of suspension, DMF was selected as the dispersed solvent to explore the potential fluorescence sensing performances for detecting NAEs and metal ions.

The NAEs, such as 2-nitrotoluene, 2, 6-dinitrotoluene, 3-nitrotoluene, p-nitrotoluene, 2,4-dinitrotoluene, trinitrophenol (TNP) and trinitrotoluene (TNT), can cause environmental pollution and explosion in chemical industry. Therefore, it is crucial that fast and effective detection of NAEs. In order to study the sensing ability of compound **1** towards many NAEs, fluorescence titration experiments were carried out by gradual addition of 1 mM solutions of various NAEs. As shown in Figs. 3 and 4, 2,6-DNT, NB partially affect the emission intensities; 2,4-DNT, 4-NT, 3-NT, 2-NT have medium affection for the emission intensities. Furthermore, after adding TNP, the emission spectrum exhibits red shift of 20 nm compared to complex **1**, showing the existence of noncovalent H-bonding interaction between -NH_2 and TNP. which can be certified by IR spectra of complex **1** and **1**-TNP, the vibration position of –NH_2 in **1**-TNP exhibits a bit change compare with complex **1** (Fig. S6). Interestingly, such H-bonding interaction didn't enhance the quenching effect [19]. While the emission spectra exhibit a bit blue

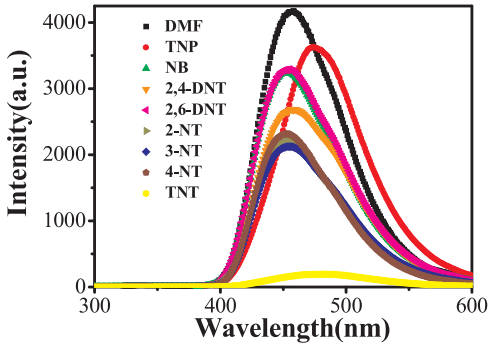

Fig. 3. The fluorescence intensities of compound **1** dispersed in different NEs solutions (1 mM).

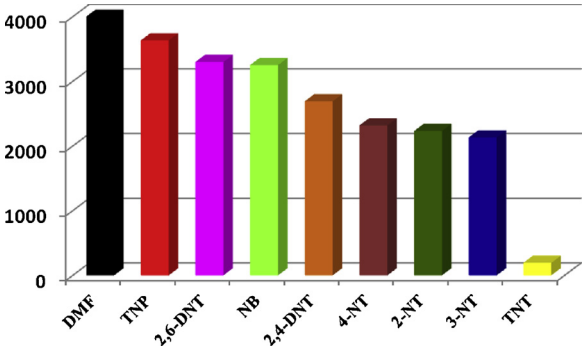

Fig. 4. The fluorescence intensities of **1** dispersed in 0.091 mM different DMF solutions of NAEs.

shift after adding other NAEs, which are attributed to tightly stacking and tiny perturbation of NAEs. Interestingly, the emission intensity was rapidly and completely quenched when TNT solution was added. Moreover, the TNT induced fluorescence quenching of **1** can be easily distinguished by the naked eye using a hand-held UV lamp (λ_{max} = 365 nm) (Fig. 5), demonstrating the applicability of **1** for real-time detection of TNT.

To further understand the luminescent quenching degree, the quenching curves were quantitatively studied by Stern-Volmer equation (S-V plot): $I_0/I = 1 + K_{sv} \times [M]$. The results reveal that fluorescence intensities were significantly decreased when TNT acted as quencher, the S-V plots exists a good linear relationship between the luminescence intensities and the low concentration of TNT (0–2.5 × 10^{-4} M), and correlation coefficient is up to 0.994. Whereas the S-V curve subsequently deviates from the linear relationship at higher concentrations. According to the S-V equation, the K_{sv} value is up to 0.58 × 10^4 M^{-1} for TNT (Fig. 6a–c). To best of our knowledge, the K_{sv} in this work is larger than most of LMOFs sensors for TNT in Table 1. Further detailed analysis denotes that the detection limits for TNT and Cr^{3+} are 0.12 and 0.01 μmol L^{-1} for **1**, respectively, according to 3δ/k (δ: standard error; k: slope) (Table S3). The detection linear range of **1** for TNT and Cr^{3+} are 0.12–148 μmol L^{-1} and 0.01–291 μmol L^{-1}. To further investigate the quenching selectivity of TNT to other NAEs, the luminescent intensities were investigated in the presence of other NAEs. The results indicate that the fluorescence intensities are still decreased significantly in various NAEs solutions of DMF with concentration of 1 × 10^{-2} M when TNT acted as a quencher (Fig. S7). Thus complex **1** can be used as an excellent fluorescence sensor for selectively detecting TNT. Additionally, the recyclable performance of **1** in TNT was also investigated, complex **1** can be readily regenerated by washing with DMF several times (Fig. 7), the results show that after five recycles, the fluorescence intensities were not significantly reduced. The PXRD spectrum (Fig. S8) of the sample after five times recycled in TNT solution was measured to confirm the stability of **1**. To best our knowledge, it hasn't been found yet that Mg-MOFs act fluorescent probes for selective detecting TNT, furthermore, complex **1** is also the first LMOF sensor for high selective detecting TNT. The difference between the

Fig. 5. Upon the addition of various nitro explosives solution (150 μL each) in DMF suspension of **1** under UV light (λ_{max} = 365 nm).

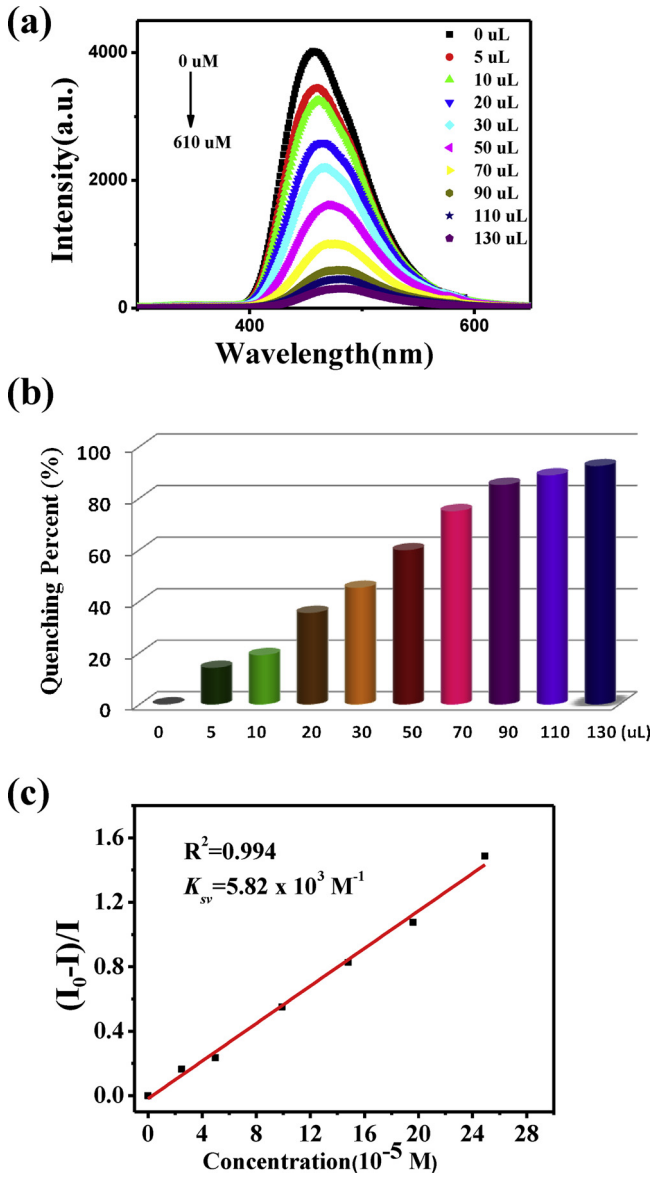

Fig. 6. (a) Fluorescence spectra of **1** with different amounts of TNT; (b) Quenching percentages when adding different concentrations of TNT; (c) S-V plot of **1** dispersed in different concentrations of TNT.

Table 1
A comparison of MOF-based luminescent probes for the detection of TNT.

Complexes	K_{sv} (M^{-1})	Detection Limit	Ref.
$\{(Me_2NH_2)_{10}[Zn_6L_4(O_3)_2Zn_3]\cdot G_x\}_n$	3.83×10^3	_	[24]
TB-Zn-CP	1.09×10^3	_	[25]
PCN-224	3.5×10^4	50 μM	[26]
TMU-32	3.06×10^3	_	[27]
TMU-31	5.58×10^3	_	[27]
Fe_3O_4@Tb-BTC	9.48×10^4	_	[28]
$[Zn_2(NDC)_2(bpy)]\cdot G_x$	4.5×10^3	_	[29]
$[Mg(ATDC)(H_2O)_2]_n$	0.58×10^4	0.12μM	This work

quenching mechanisms can be predicted by the fluorescence lifetime of the fluorophore in the presence of quencher. As shown in Fig. S9, the average excited state lifetime (τ) of **1** were 0.58 and 1.39 ns, respectively, before and after the addition of 130 μLTNP. These average life values indicate that the quenching process is essentially dynamic in nature. The fluorescence quantum yields are 1.17% for complex **1** and 2.47% for complex **1** + **TNT** (Fig. S10).

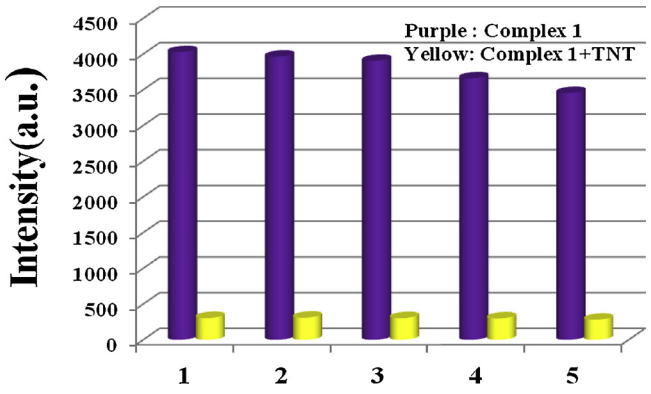

Fig. 7. Five recycle tests of complex **1** for sensing TNT.

According to previous studies, there are three mainly possible quenching mechanisms for NAEs, the structural collapse or transformation, the photo-induced electron transfer (PET) from the CB(conduction band) of Mg-MOF to the LUMO(lowest unoccupied molecular orbital) of TNT, resonance energy transfer (RET) between the absorption spectrum of the TNT and the fluorescence excitation/emission spectrum of Mg-MOF, or the combination. The structural collapse or transformation could be excluded because XRD patterns of the recycled samples reveals that the crystal structure is still maintained after sensing experiments (Fig. S8). From the HOMO and LUMO orbital energies of electron-deficient NEs as calculated by density functional theory at the B3LYP/6-31g* level, the electron can be transferred easily from the CB band of **1** to the LUMO of NEs under excitation, resulting in the fluorescence quenching, thus indicating the existence of PET. To demonstrate the overlap of spectrum exists in the sensing process, the UV − vis spectra of various NAEs dispersed in DMF were investigated, the results display that the wide absorption bands obviously exist at 300–500 nm, which can easily overlap with the fluorescence excitation/emission peaks of Mg-MOF; especially for TNT, showing partly overlap and resulting in great luminescence quenching as well (Fig. S11) [30–35]. Besides, XPS spectra were also employed to provide more information on the interactions between $-NH_2$ and TNT. As shown in Fig. 8, the $-NH_2$ (N1s) peaks of **1**-TNT (399.0 ev) have not show significant change compare with $-NH_2$ (N1s) of complex **1** (398.8 ev), showing that no obvious chemical interactions were found between $-NH_2$ and TNT, the IR spectra of **1** and **1**-TNT show the vibration peaks of $-NH_2$ (3200–3500 cm^{-1}) have not obviously change as well, so the chemical interactions between the -NH_2 and TNT could be excluded (Fig. S6). Given all this, indicating that the electron and energy transfer play key roles for the fluorescence quenching.

To investigate the fluorescence sensing performances of complex **1** to various metal ions, complex **1** was dispersed in various 1×10^{-3} M DMF solutions of metal ions $M(NO_3)_n$ (M = Na^+, Pb^{2+}, Li^+, Ca^{2+}, Ag^+, Cr^{3+}, Zn^{2+}, Cd^{2+}, Ni^{2+}, Cu^{2+}, Co^{2+}, Mn^{2+}), then the fluorescence sensing experiments were studied under excitation at 290 nm. As shown in Fig. S12, the fluorescence intensity of the suspension was almost drastically and rapidly quenched when Cr^{3+} ions was added, the Cu^{2+} and Hg^{2+} partially affect the emission intensities, while other metal ions haven't obviously effect on the emission intensities. Such distinct quenching effects, especially Cr^{3+} ion, indicate that **1** could be utilized as a fluorescence sensing probe to detect Cr^{3+} ions with high selectivity and sensitivity. Thus, to further explore the sensitivity of **1** as Cr^{3+} sensor, the fluorescence titrations were examined by changing the concentrations of Cr^{3+} to investigate the quenching behavior. As shown in Fig. 9a, the fluorescence intensities of **1** are gradually weaken when the amount of 1×10^{-2} M Cr^{3+} ions were increased, and the fluorescence intensity was quenched more than 90% when the concentration of Cr^{3+} is up to 0.29 mM (60 u L)(Fig. 9b). The Stern-Volmer plot for Cr^{3+} exhibited a good liner correlation (R^2 = 0.998) at low

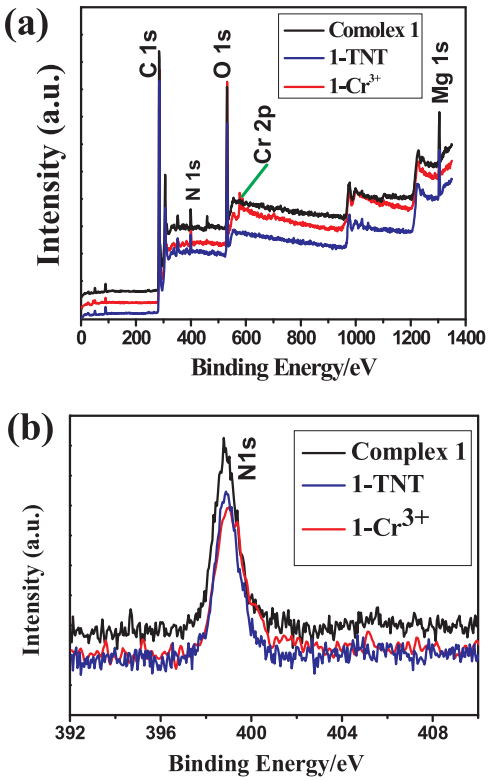

Fig. 8. (a) XPS survey spectra of **1**, **1**-TNT and **1**-Cr^{3+}; (b) N1s XPS spectrum of **1**, **1**-TNT and **1**-Cr^{3+}. (**1** dispersed in 10^{-2} M TNT or Cr^{3+} and dried in air).

concentrations (0–3.5 × 10^{-5} M), the value of K_{sv} is estimated to be as high as 4.32 × 10^5 M^{-1} (Fig. 9c). To further study whether other metal ions can disturb the quenching selectivity of Cr^{3+}, the luminescent intensities were investigated with the existence of other metal ions. The results show that when Cr^{3+} ion was gradient added into various metal ions solutions of DMF with concentration of 1 × 10^{-3} M acted as a quencher, the fluorescence intensities also significantly decreased, even for Cu^{2+} ion, the quenching effect is still pretty obvious. Which indicates that complex **1** has high selectivity for detecting Cr^{3+} (Fig. S13).

To best our knowledge, only one Mg-MOF was acted as fluorescent probes for detecting Cr^{3+} ions $[CH_3\text{-dpb}]_2[Mg_3(1,4\text{-NDC})_4(\mu\text{-}H_2O)_2(CH_3OH)(H_2O)]\cdot 1.5H_2O$ (1,4-H_2NDC = 1,4-naphthalene dicarboxylic acid, dpb = 1,4-bis(pyrid-4-yl)benzene), complex **1** is the second Mg-MOF act as fluorescent probes for sensing Cr^{3+}, and the K_{sv} value is up to 4.32 × 10^5 M^{-1}, greater than the reported value of 1.5 × 10^4 M^{-1} [10]. Actually, this detecting result is the most excellent among all the LMOFs for detecting Cr^{3+}, and the comparisons are listed in Table 2. In addition, in order to confirm the recyclability of complex **1**, the dispersed solution was centrifuged. As shown in Fig. 10, complex **1** can restored and recycled at least four times. At the same time, PXRD pattern of the original is completely consistent with the recycled samples, showing the high stability (Fig. S8). These results prove that complex **1** is a very ideal fluorescent probe for detecting Cr^{3+} ions.

Similarly, according to previous reports and our studies, there are several reasons that metal cations cause the luminescence quenching: the ionic exchange, the collapse or change of the structure, and the competitive photon absorption between the adsorbed ions and MOFs [39]. In this case, it is sure that the fluorescence quenching of **1** neither attributed to the structural decomposition nor cationic exchange process, because the PXRD pattern of **1** recycled from Cr^{3+} solution was almost unaffected compared to the simulated patterns. Thus, such fluorescence quenching is considered to be caused by the wide absorption between 350 nm and 600 nm of Cr^{3+} (Fig. S14). Which cover

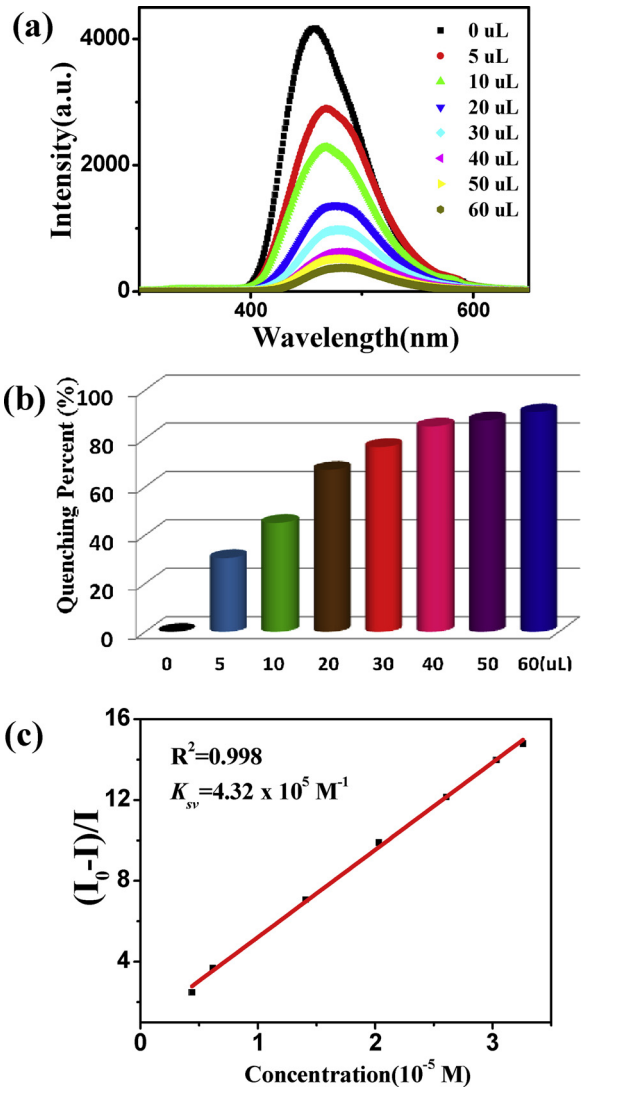

Fig. 9. (a) The changes of fluorescence intensities of complex **1** when adding various volume of 1 × 10^{-2} M Cr^{3+} ions. (b) Quenching percentages of **1** upon addition of different volumes of 1 × 10^{-2} M Cr^{3+} ions. (c) Stern-Volmer plot of **1** at different concentrations of Cr^{3+} ions.

Table 2
The quenching constants of the reported LMOFs for Cr^{3+} in suspensions.

Complexes	K_{sv}/M^{-1}	Ref.
$[Mg(ATDC)_4(H_2O)_2]$	4.32 × 10^5	This work
$[Me_2NH_2]_4[Zn_6(qptc)_3(trz)_4]\cdot 6H_2O$	4.39 × 10^4	[4]
$[CH_3\text{-dpb}]_2[Mg_3(1,4\text{-NDC})_4(u\text{-}H_2O)_2(CH_3OH)(H_2O)]\cdot 1.5H_2O$	1.5 × 10^4	[10]
$[Zn(L)(H_2O)]\cdot H_2O$	2.03 × 10^4	[12]
$[Tb(TBOT)(H_2O)](H_2O)_4(DMF)(NMP)_{0.5}$	1.36 × 10^4	[37]
Zn-MOF	5.1 × 10^4	[38]
$[Eu_2(tpbpc)_4\cdot CO_3\cdot 4H_2O]\cdot DMF$	5.14 × 10^2	[39]

the emission of Mg-MOF at 400–600 nm and hinder the absorption of Mg-MOF upon excitation, and lead to the quenching of the fluorescence [36–41].

XPS spectra were checked and demonstrate that the N1s (-NH_2) peaks of **1**-Cr^{3+} (399.0ev) have not significant change compare with the N1s (-NH_2) of complex **1** (398.8ev) (Fig. 8). The IR spectra of **1** and **1**-Cr^{3+} show that the vibration peaks of –NH_2 (3200–3500 cm^{-1}) have not obviously change as well, so the interactions between the free Lewis

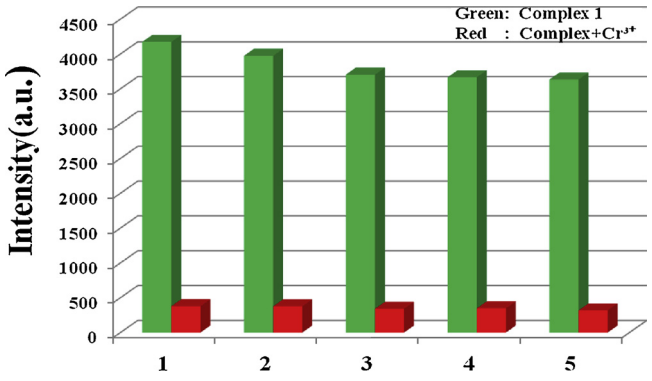

Fig. 10. Five cycle tests of **1** for sensing Cr^{3+} (bottom) cations.

base sites of -NH_2 and Cr^{3+} could be excluded (Fig. S6). The existing of trace Cr^{3+} is due to the absorption of complex **1**, which hasn't been further washed.

4. Conclusions

In summary, a novel 3D Mg-MOF $[Mg(ATDC)(H_2O)_2]_n$ (**1**) has been synthesized and characterized, complex **1** presents a pH and thermo stability fluorescent Mg-MOF sensor exhibiting highly selectivity for TNT and highly sensitivity for Cr^{3+}. Furthermore, complex **1** can be quickly regenerated by simple wash with DMF, exhibiting good recyclability for detecting TNT and Cr^{3+}. Most importantly, the Mg-MOF is the first example for selectively detecting TNT, and also has the highest sensitivity for quantitative detecting Cr^{3+}. These results prove that LMOFs with excellent performance can be rationally designed by importing applicable ligands and metal ions. Future study will be focused on the preparations of new highly selective and sensitive Mg-MOF sensors and further understanding of relationships between the structures and properties.

Ackonwledgments

This work thanks for the supports of the Natural Science Foundation of China (21501002, 21671004), Open Fundation of the Key Laboratory of Photochemical Conversion and Optoelectronic Material, TIPC, CAS; Open Fundation of the Key Lab of Photovoltaic and Energy Conservation Materials.

CCDC 1845260.

Appendix A. Supplementary data

Supplementary material related to this article can be found, in the online version, at doi:https://doi.org/10.1016/j.snb.2018.12.022.

References

[1] Y.J. Deng, N.J. Chen, Q.Y. Li, X.J. Wu, X.L. Huang, Z.H. Lin, Y.G. Zhao, Highly fluorescent metal–organic frameworks based on a benzene-cored tetraphenylethene derivative with the ability to detect 2,4,6-trinitrophenol in water, Cryst. Growth Des. 17 (2017) 3170–3177.

[2] R. Lv, J.Y. Wang, Y.P. Zhang, H. Li, L.Y. Yang, S.Y. Liao, W. Gu, X. Liu, An amino-decorated dual-functional metal–organic framework for highly selective sensing of Cr(III) and Cr(VI) ions and detection of nitroaromatic explosives, J. Mater. Chem. A Mater. Energy Sustain. 4 (2016) 15494–15500.

[3] J.N. Xiao, J.J. Liu, X.C. Gao, G.F. Ji, D.B. Wang, Z.L. Liu, A multi-chemosensor based on Zn-MOF: ratio-dependent color transition detection of Hg (II) and highly sensitive sensor of Cr (VI), Sens. Actuators B Chem. 269 (2018) 164–172.

[4] X.X. Jia, R.X. Yao, F.Q. Zhang, X.M. Zhang, A fluorescent anionic MOF with $Zn_4(trz)_2$ chain for highly selective visual sensing of contaminants: Cr(III) Ion and TNP, Inorg. Chem. 56 (2017) 2690–2696.

[5] S.J. Dong, J.S. Hu, K. Wu, M.D. Zheng, A Mg(II)-MOF as recyclable luminescent sensor for detecting TNP with high selectivity and sensitivity, Inorg. Chem. Commun. 95 (2018) 111–116.

[6] Y.X. Gao, G. Yu, K. Liu, B. Wang, Luminescent mixed-crystal Ln-MOF thin film for the recognition and detection of pharmaceuticals, Sens. Actuators B Chem. 257 (2018) 931–935.

[7] T. Zhang, K. Manna, W. Lin, Metal-organic frameworks stabilize solution-inaccessible cobalt catalysts for highly efficient broad-scope organic transformations, J. Am. Chem. Soc. 138 (2016) 3241–3249.

[8] B. Amlan, Y. Muhammed, S. Manabendra, B. Shyam, 3D luminescent amide-functionalized cadmium tetrazolate framework for selective detection of 2,4,6-trinitrophenol, Cryst. Growth Des. 16 (2016) 842–851.

[9] W. Liu, X. Huang, C. Xu, C.Y. Chen, L.Z. Yang, W. Dou, W.M. Chen, H. Yang, W.S. Liu, A multi-responsive regenerable europium-organic framework luminescent sensor for Fe^{3+}, Cr(VI) anions, and picric acid, Chem. Eur. J. 22 (2016) 18769–18776.

[10] Z.F. Wu, L.K. Gong, X.Y. Huang, A Mg-CP with in situ encapsulated photochromic guest as sensitive fluorescence sensor for Fe^{3+}/Cr^{3+} ions and nitro-explosives, Inorg. Chem. 56 (2017) 7397–7403.

[11] Y. Shen, C.C. Fan, Y.Z. Wei, J. Du, H.B. Zhu, Y. Zhao, Construction of non-interpenetrating and interpenetrating (4-Fold and 8-Fold) 3-D Cd(II) networks with tris(1,2,4-triazol-4-yl)phenyl)amine modulated by aromatic dicarboxylate coligands, Cryst. Growth Des. 16 (2016) 5859–5868.

[12] X.Y. Guo, F. Zhao, J.J. Liu, Z.L. Liu, An ultrastable zinc(II)-organic framework as a recyclable multi-responsive luminescent sensor for Cr(III), Cr(VI) and 4-nitrophenol in the aqueous phase with high selectivity and sensitivity, J. Mater. Chem. A 5 (2017) 20035–20043.

[13] S.D. Li, L.P. Liu, M.L. Zhu, C.X. Yuan, S.S. Feng, A bifunctional chemosensor for detection of volatile ketone or hexavalent chromate anions in aqueous solution based on a Cd(II) metal–organic framework, Sens. Actuators B Chem. 258 (2018) 970–980.

[14] B. Minoo, Y.M. Mohammad, M. Ali, S. Alexander, Two dimensional host-guest metal-organic framework sensor with high selectivity and sensitivity to picric acid, ACS Appl. Mater. Inter. 8 (2016) 21472–21479.

[15] D. Yue, D. Zhao, J. Zhang, L. Zhang, K. Jiang, X. Zhang, Y.J. Cui, Y. Yang, B.L. Chen, G.D. Qian, A luminescent cerium metal–organic framework for the turn-on sensing of ascorbic acid, Chem. Commun. 53 (2017) 11221–11224.

[16] M. Wang, X. Liu, H. Lu, H. Wang, Z. Qin, Highly selective and reversible chemosensor for Pd^{2+} detected by fluorescence, colorimetry, and test paper, ACS Appl. Mater. Interfaces 7 (2015) 1284–1289.

[17] S.N. Sanjog, J. Biplab, K.C. Abhijeet, M. Soumya, K.G. Sujit, Highly selective detection of nitro explosives by a luminescent metal-organic framework, Angew. Chem. Int. Ed. 125 (2013) 2953–2957.

[18] J. Wang, C. Liang, W. Lin, Significantly enhanced photocatalytic hydrogen evolution under visible light over CdS embedded on metal-organic frameworks, ACS Catal. 2 (2017) 2630–2640.

[19] B. Gole, A.K. Bar, P.S. Mukherjee, Fluorescent metal-organic framework for selective sensing of nitroaromatic explosives, Chem. Commun. 47 (2011) 12137–12139.

[20] Y.L. Hu, M.L. Ding, X.Q. Liu, L.B. Sun, H.L. Jiang, Rational synthesis of an exceptionally stable Zn(II) metal-organic framework for the highly selective and sensitive detection of picric acid, Chem. Commun. 52 (2016) 5734–5737.

[21] N. Gao, Y.F. Zhang, P.C. Huang, Z.H. Xiang, F.Y. Wu, L.Q. Mao, Perturbing tandem energy transfer in luminescent heterobinuclear lanthanide coordination polymer nanoparticles enables real-time monitoring of release of the anthrax biomarker from bacterial spores, Anal. Chem. 90 (2018) 7004–7011.

[22] L.N. Li, S.S. Shen, R.Y. Lin, Y. Bai, H.W. Liu, Rapid and specific luminescence sensing of Cu(II) ions with a porphyrinic metal-organic framework, Chem. Commun. 53 (2017) 9986–9989.

[23] S.J. Dong, J.S. Hu, X.L. Zhang, M.D. Zheng, A bifunctional Zn(II)-MOF as recyclable luminescent sensor for detecting TNT and Fe^{3+} with high selectivity and sensitivity, Inorg. Chem. Commun. 97 (2018) 180–186.

[24] X.S. Wang, L. Li, D.Q. Yuan, Y.B. Huan, R. Cao, Fast, highly selective and sensitive anionic metal-organic framework with nitrogen-rich sites fluorescent chemosensor for nitro explosives detection, J. Hazard. Mater. 344 (2018) 283–290.

[25] S. Shanmugaraju, C. Dabadie, K. Byrne, A.J. Savyasachi, D. Umadevi, W. Schmitt, J.A. Kitchen, T. Gunlaugsson, A supramolecular Tröger's base derived coordination zinc polymer for fluorescent sensing of phenolic-nitroaromatic explosives in water, Chem. Sci. 8 (2017) 1535–1546.

[26] J. Yang, Z. Wang, K.L. Hu, Y.S. Li, J.F. Feng, J.L. Shi, J.L. Gu, Rapid and specific aqueous-phase detection of nitroaromatic explosives with inherent porphyrin recognition sites in metal-organic frameworks, ACS Appl Mater. Interface 7 (2015) 11956–11964.

[27] A.A. Tehrani, L.L. Esrafili, S. Abedi, A. Morsali, L. Carlucci, D.M. Proserpio, J. Wang, P.C. Junk, T.F. Liu, Urea metal-organic frameworks for nitro-substituted compounds sensing, Inorg. Chem. 56 (2017) 1446–1454.

[28] J.J. Qian, L.G. Qiu, Y.M. Wang, Y.P. Yuan, A.J. Xie, Y.H. Shen, Fabrication of magnetically separable fluorescent terbium-based MOF nanospheres for highly selective trace-level detection of TNT, Dalton Trans. 43 (2014) 3978–3983.

[29] K.S. Asha, K. Bhattacharyyab, S. Mandal, Discriminative detection of nitro aromatic explosives by a luminescent metal-organic framework, J. Mater. Chem. C Mater. Opt. Electron. Devices 2 (2014) 10073–10081.

[30] J.S. Hu, X.Q. Yao, M.D. Zhang, L. Qin, Y.Z. Li, Z.J. Guo, H.G. Zheng, Z.L. Xue, Syntheses, structures, and characteristics of four new metal-organic frameworks based on flexible tetrapyridines and aromatic polycarboxylate acids, Cryst. Growth Des. 12 (2012) 3426–3435.

[31] H.L. Jiang, H. Liu, C.Y. Xu, D.D. Li, Integration of plasmonic effects and schottky junctions into metal-organic framework composites: steering charge flow for enhanced visible-light photocatalysis, Angew. Chem. Int. Ed. 57 (2018) 1103–1107.

[32] Y.K. Che, E.G. Dustin, H.L. Huang, D.J. Yang, X.M. Yang, D. Emre, Z. Xue, H.J. Zhao, S.M. Jeffrey, L. Zang, Diffusion-controlled detection of trinitrotoluene:

interior nanoporous structure and low highest occupied molecular orbital level of building blocks enhance selectivity and sensitivity, J. Am. Chem. Soc. 134 (2012) 4978–4982.
[33] G. Bappaditya, K.B. Arun, S.M. Partha, Fluorescent metal-organic framework for selective sensing of nitroaromatic explosives, Chem. Commun. 47 (2011) 12137–12139.
[34] G.D. Zou, Z.P. Wang, Y. Song, B. Hu, X.Y. Hong, Syntheses, structures and photocatalytic properties of five new praseodymium-antimony oxochlorides: from discrete clusters to 3D inorganic-organic hybrid racemic compounds, Dalton Trans. 43 (2014) 10064–10073.
[35] S. Homayoonnia, S. Zeindi, Design and fabrication of capacitive nanosensor based on MOF nanoparticles as sensing layer for VOCs detection, Sens. Actuators B Chem. 237 (2016) 776–786.
[36] Z. Sun, M. Yang, Y. Ma, L.C. Li, Multi-responsive luminescent sensors based on two-dimensional lanthanide–metal organic frameworks for highly selective and sensitive detection of Cr(III) and Cr(VI) ions and benzaldehyde, Cryst. Growth Des. 17 (2017) 4326–4335.
[37] T.Y. Gu, M. Dai, J.Y. David, Z.G. Ren, J.P. Lang, Luminescent Zn(II) coordination polymers for highly selective sensing of Cr(III) and Cr(VI) in water, Inorg. Chem. 56 (2017) 4668–4678.
[38] J.J. Liu, G.F. Ji, J.N. Xiao, Z.L. Liu, Ultrastable 1D europium complex for simultaneous and quantitative sensing of Cr(III) and Cr(VI) ions in aqueous solution with high selectivity and sensitivity, Inorg. Chem. 56 (2017) 4197–4205.
[39] K.S. Debal, M. Partha, Highly selective and sensitive luminescence turn-on-based sensing of $Al3+$ ions in aqueous medium using a MOF with free functional sites, Inorg. Chem. 54 (2015) 6373–6379.
[40] X.J. Hong, Q. Wei, Y.P. Cai, S.R. Zheng, Y. Yu, Y.Z. Fan, X.Y. Xu, L.P. Si, 2-Fold interpenetrating bifunctional Cd-metal-organic frameworks: highly selective adsorption for CO_2 and sensitive luminescent sensing of nitro aromatic 2,4,6-trinitrophenol, ACS Appl. Mater. Inter. 9 (2017) 4701–4708.
[41] K. Zheng, Z.Q. Liu, Y. Huang, F. Chen, C.H. Zeng, S.J. Zhong, S.W. Ng, Highly luminescent Ln-MOFs based on 1,3-adamantanediacetic acid as bifunctional sensor, Sens. Actuators B Chem. 257 (2018) 705–713.